

# Rapid Concentration of Nanoparticles with DC Dielectrophoresis in Focused Electric Fields

Dafeng Chen · Hejun Du · Chee Yong Tay

Received: 24 August 2009 / Accepted: 18 September 2009 / Published online: 1 October 2009  
© to the authors 2009

**Abstract** We report a microfluidic device for rapid and efficient concentration of micro/nanoparticles with direct current dielectrophoresis (DC DEP). The concentrator is composed of a series of microchannels constructed with PDMS-insulating microstructures for efficiently focusing the electric field in the flow direction to provide high field strength and gradient. The location of the trapped and concentrated particles depends on the strength of the electric field applied. Both ‘streaming DEP’ and ‘trapping DEP’ simultaneously take place within the concentrator at different regions. The former occurs upstream and is responsible for continuous transport of the particles, whereas the latter occurs downstream and rapidly traps the particles delivered from upstream. The performance of the device is demonstrated by successfully concentrating fluorescent nanoparticles. The described microfluidic concentrator can be implemented in applications where rapid concentration of targets is needed such as concentrating cells for sample preparation and concentrating molecular biomarkers for detection.

**Keywords** Microfluidics · DC dielectrophoresis · Nanoparticles · Electrokinetics

## Introduction

The ability to concentrate or extract micro/nanoparticles, such as cells, viruses, bacteria, and DNA, from the

background matrix is essential to many biomedical applications. The form of these particles in high concentration facilitates the subsequent analytical and processing steps. For example, current methods in microbial analysis of water quality require subpopulations (e.g. *E. coli*) sampled in detectable levels of concentration [1]. In the process of gene hybridization, rates can be accelerated by concentration of single-stranded DNA. The sensitivity of fluorescence-based bioassays is greatly improved with pre-concentrated labeled targets. In recent years, more and more biological and chemical assays are conducted in microscale devices with the rapid development of micrototal analysis systems ( $\mu$ -TAS) [2]. Traditional methods of concentrating samples by centrifuging and subsequently removing the supernatant are not amenable to the format of microchips. A number of methods have been reported concerning on-chip microfluidic concentration and manipulation of micro/nanoparticles such as dielectrophoresis [3–5], optical tweezers [6], and ultrasonic wave [7]. They are readily integrated into microdevices by patterning micro/nanometal electrodes (in the case of dielectrophoresis) or using remote manipulation with laser or ultrasound.

We report here a direct current dielectrophoresis-based method for rapid concentration of nanoparticles in a microfluidic device. Dielectrophoresis (DEP) is the motion of a particle in a non-uniform electric field due to the unbalanced electrostatic forces on the particle’s induced dipole [8]. This phenomenon has been widely used for concentration, manipulation, separation, sorting, and transport of particles such as beads, bacteria, and cells [3–5, 9–12]. The majority of these applications employ AC electric fields generated by closely spaced microelectrode arrays that are generally constructed with MEMS-based microfabrication techniques. AC fields promote lower electrode polarization and electrophoretic effects. However,

---

D. Chen (✉) · H. Du · C. Y. Tay  
School of Mechanical & Aerospace Engineering,  
Nanyang Technological University, 50 Nanyang Avenue,  
Singapore 639798, Singapore  
e-mail: dfchen@pmail.ntu.edu.sg

AC DEP faces certain issues that limit its applications, such as electrode fouling and electric field decay above the microelectrodes. An alternative to AC dielectrophoresis is the insulator-based DEP (iDEP) or DC DEP [5, 13, 14], in which no metal microelectrodes are embedded in the chip and DC electric fields are applied from an external electrode pair. This simplifies the fabrication of microdevices by eliminating the metal deposition processes. Insulator structures are robust and chemically inert. Effects such as electrochemical reactions and electrolysis observed in AC DEP are less likely to occur in iDEP. Cummings and Singh observed two flow regimes in insulator-based DEP: (1) ‘streaming DEP’ where streams of highly concentrated and rarified particles were created between the insulating posts at relatively low voltages and (2) ‘trapping DEP’ where particles were trapped around the insulating posts at higher voltages [15]. These observations lead to potential applications, for example, streaming DEP can be used to focus and transport particles, and trapping DEP can be used for particle concentration and filtration. The mechanics behind the phenomenon is the competition between electrokinetic (electrophoresis and electroosmosis) and dielectrophoretic forces [15]. The former is linearly proportional to the electric field, while the latter is proportional to the field squared. At low voltages, electrokinetic flow is dominant over DEP and diffusion, resulting in the regime of streaming DEP. At higher voltages, DEP is dominant, resulting in trapping DEP. This letter describes an insulating microstructure that is designed to highly focus and thus ‘amplify’ the electric field. Upon the application of voltage, the generated electric field is focused in the direction of fluid flow. Trapping DEP first occurs at these field-focused areas located at the downstream, while streaming DEP occurs upstream and continuously transports and delivers the particles. The described setup is capable of rapidly concentrating and collecting nanoparticles from continuous flow that is driven by electroosmosis.

## Materials and Methods

### The Microstructure for Field Focusing

In the case of DC DEP, the non-uniformity of electric field is generally created by embedded obstacles such as a specifically arranged array of insulators. Delicately designed insulators lead to useful distribution of the electric field as well as the resulting electrostatic forces that are associated with the field, such as DEP, electrophoretic, and electroosmotic forces. The proposed microdevice is composed of a delicate insulating structure constructed in a channel for the purpose of field focusing (Fig. 1). A simple and effective field-focusing insulator structure is shown in Fig. 1a, which

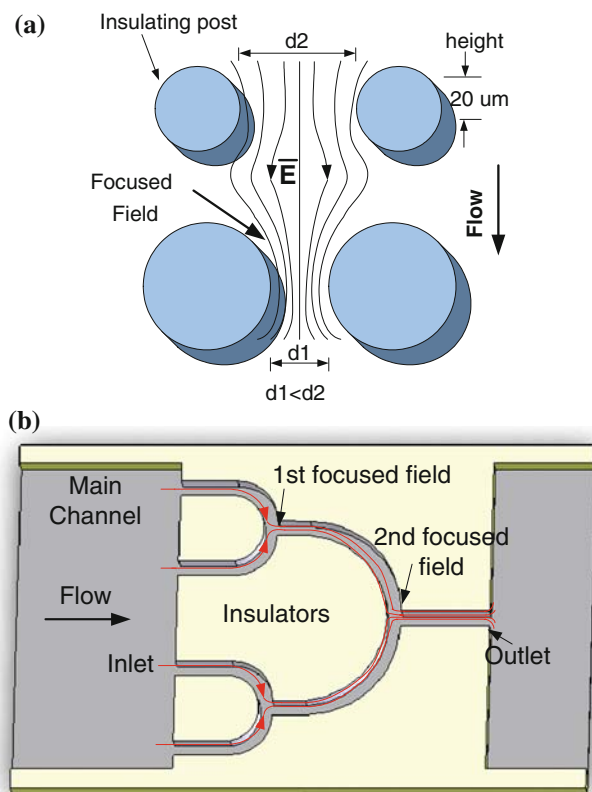


**Fig. 1** **a** Diagram of a simple design for field focusing via insulator posts. The electric field ( $E$ ) is indicated with field lines. **b** An insulating ‘tree’ structure for rapid electric field focusing

is formed by an array of circular posts spaced by different distances ( $d1 < d2$ ). An electric field is generally applied externally from the two electrodes (anode and cathode, respectively) located at opposite ends of the channel. Upon the application of the field, a non-uniform distribution is generated along the insulators, as indicated by the field lines. Depending on the patterns of the insulators, the field is relatively concentrated in certain areas. ‘Field-focused’ areas are of higher non-uniformity compared to the ‘unfocused’ areas and therefore are more preferable for trapping DEP. Derived from the design in Fig. 1a, a more effective insulating structure is shown in Fig. 1b, which is referred to as a ‘tree system’ for field focusing. The tree system enables multilevel-focusing operations in the direction of flow (from the left to the right) at consecutive regions (as indicated with numbers 1–4). From the entry on the left to the exit on the right, the electric field gradually converges. This results in interesting movement of particles carried by the fluid flow due to the combined effects of various forces.

### Theoretical

Suspended particles in the electric field experience a number of significant forces including DEP, electrophoretic, and

electro-osmotic effects. The superposition of electrophoretic and electroosmotic transport is generally termed electrokinetic flow. The resulting motion of the particle is determined by the superposed electrokinetic velocity [15]

$$u_{ek} = \mu_{ek}E = u_{eo} + u_{ep} = (\mu_{eo} - \mu_{ep})E \quad (1)$$

where  $\mu_{ek}$ ,  $\mu_{eo}$ , and  $\mu_{ep}$  are the electrokinetic, electroosmotic, and electrophoretic mobility, respectively.  $E$  is the electric field. Equation 1 indicates that the electrokinetic motion of the particles is linearly proportional to the local electric field. Under ideal electrokinetic flow, particles flow along the electric field lines, and no concentration of particles occurs.

On the other hand, dielectrophoretic velocity,  $u_{dep}$ , which is induced by the dielectrophoretic force in a non-uniform field, is proportional to the gradient of the electric field [8]

$$u_{dep} = \mu_{dep} \nabla(E \cdot E) \quad (2)$$

where  $\mu_{dep}$  is the dielectrophoretic mobility.

In contrast to electrokinetic flow, dielectrophoretic motion is along the electric field gradient, and the transport can result in concentration, focusing, or trapping of particles in non-uniform fields. Such field gradients are readily produced either by embedded metal electrodes in the case of AC dielectrophoresis or by insulating posts within the channel exposed to an external electric field. Dependent on the polarizability of the particles and suspended medium, positive DEP (drawing particles to field maximum) or negative DEP (repelling particles from field maximum) takes place [8].

The above equations imply that the resulting particle movement depends on the relative strengths of electrokinetic and dielectrophoretic effects. As discussed in Ref. [15], above a threshold electric field, DEP becomes dominant over electrokinetic and diffusion effects. Particles will be trapped and concentrated dielectrophoretically, and this regime is called ‘trapping DEP’. In this work, we proposed a field-focusing structure (Fig. 1b) in which rapid electric field gradients are generated to readily induce ‘trapping DEP’. Electrokinetic flow is responsible for

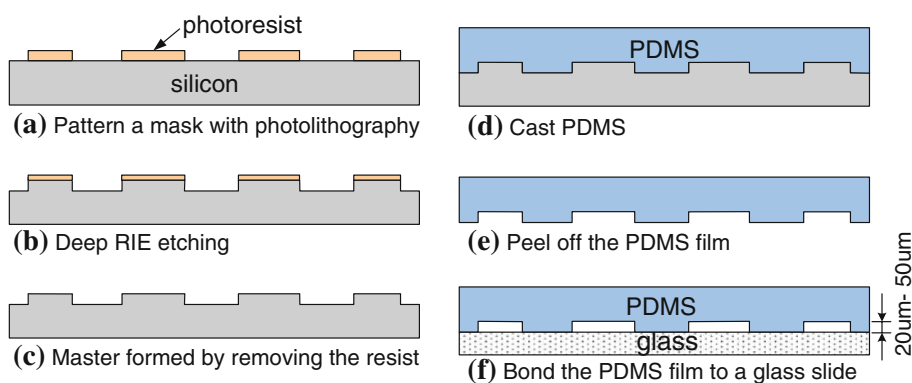
particle transport, while dielectrophoresis is responsible for local particle trapping.

### Microfabrication and Experimental Setup

The microfluidic device containing the insulating microelectrodes was fabricated using conventional microfabrication techniques (Fig. 2). The PDMS (polydimethylsiloxane)-insulating microstructures were manufactured by casting from a microfabricated silicon master. To fabricate the master, a 10  $\mu\text{m}$  thick layer of photoresist (AZ9260, Clariant, Somerville, NJ) was spun and patterned on a 4-inch wafer with a photolithography process (Fig. 2a). The patterned photoresist served as the mask for the subsequent process of deep reactive ion etching (DRIE). To form the complementary patterns in the master, an ICP (inductively coupled plasma) deep RIE process was applied (Surface Technology Systems plc, Newport, UK). The etching rate was about 3  $\mu\text{m}/\text{min}$  with a gas recipe of 115-sccm  $\text{SF}_6$  + 13-sccm 150  $\text{O}_2$  + 100-sccm  $\text{C}_4\text{F}_8$  at a cycling of 8 s passivation and 13 s etching. Patterns of depth of 20–50  $\mu\text{m}$  were fabricated (Fig. 2b, c). The master surface was then passivated with gas  $\text{C}_4\text{F}_8$  for 5 min. The passivation reduced the adhesion of PDMS to the master surface and in turn facilitated the subsequent PDMS peeling-off step. PDMS mixture was then poured onto the master and incubated at room temperature overnight (Fig. 2d). The cured PDMS film was peeled off from the master, and the insulating microstructures were formed on the PDMS film (Fig. 2e). To construct an enclosed microfluidic device containing the microstructures and microchannels, the PDMS film was then bonded to a glass slide (Fig. 2f).

Figure 3a depicts a photograph of the PDMS-insulating microstructure fabricated with the process depicted in Fig. 2. Microchannels formed by the PDMS guide the EOF-driven flow from the left to the right. In the flow direction, the microchannels merge into subsequent microchannels, terminating in a single outlet at the very right. In the proposed structure, four trapping regions (indicated as ‘Region 1’–‘Region 4’) are formed. These regions have

**Fig. 2** Diagrams illustrating the fabrication of the microfluidic device containing PDMS-insulating microstructures



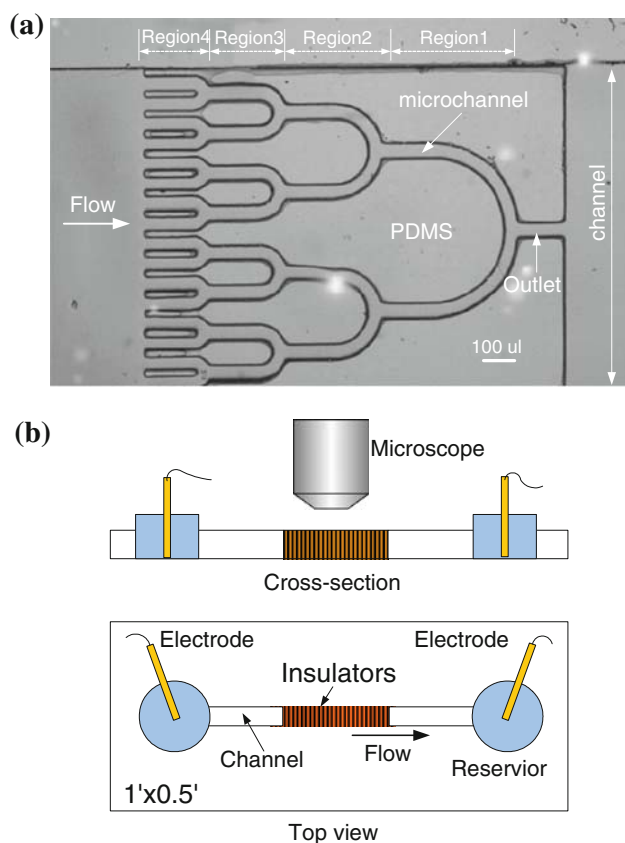


**Fig. 3** **a** Photograph of the PDMS-insulating microstructure for concentrating of particles. **b** Diagram showing the microfluidic chip and experimental setup composed of microfabricated insulators, inlet/outlet reservoirs, two electrodes, and a fluorescence microscope

been designed to effectively concentrate particles at various conditions by focusing the electric field. Figure 3b shows a top view of the completed microfluidic chip containing the microfabricated insulators and the inlet/outlet reservoirs. To generate the electric field, two Pt electrodes were vertically placed in the outlet and inlet reservoirs, respectively. In experiments, the solution containing the particles was introduced at the inlet reservoir. The liquid then automatically filled the channel due to the capillary action. The motion of particles was imaged using an epifluorescent microscope (Nikon TE2000-S).

## Results and Discussions

To investigate how the electric field is focused within the tree system, the field distribution was simulated with a finite element software (Femlab 3.2, COMSOL Inc., Burlington, MA, USA). In the simulation, the DC electric field was defined to apply from both the ends of the main channel. The simulated non-dimensional electric field ( $E$ ) distribution is shown in Fig. 4. The microstructure is

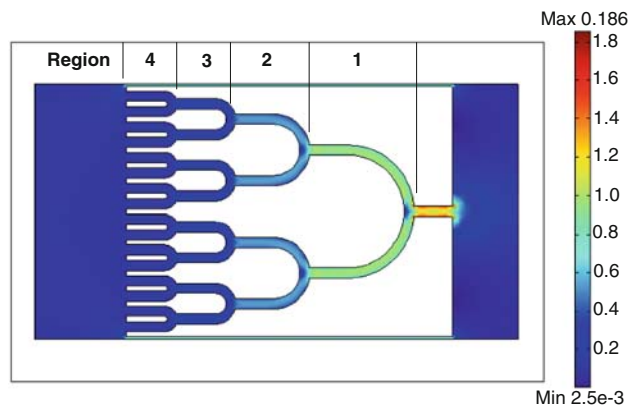


**Fig. 4** Simulated non-dimensional electric field ( $E$ ) distribution in the concentrator. The electric field is applied from the ends of the main channel

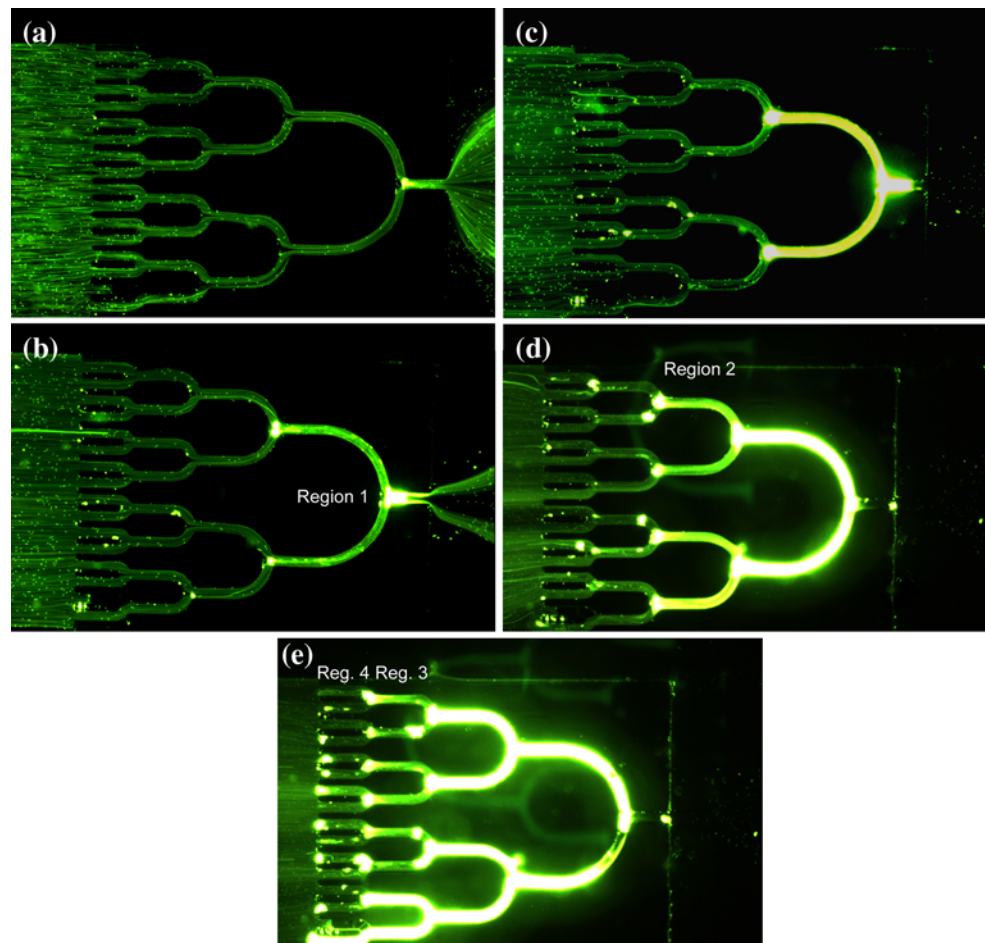
divided into four regions as indicated with '1'–'4' in the figure. From Regions 4–1, the field strength increases gradually. The insulating concentrator was designed in this way to focus the electric field in the direction of the fluid flow (from the left to the right).

The performance of the microfluidic concentrator was tested with green fluorescent polystyrene microspheres of diameter of 930 nm (Duke Scientific Co., CA, USA). The microspheres emit green light (508 nm) when they are excited by blue light (468 nm). Before use, the particles were re-suspended at low concentration in deionized water, and the conductivity of the medium was adjusted by adding phosphate buffer solution (PBS, Fisher Scientific, NJ). The conductivity was measured using a conductivity meter with graphite sensor electrodes (Dist3WP, Hanna Instruments Inc., RI). Solutions of 1.0–10.0 mS/m were used in the experiments. To begin, a suspension of fluorescent microspheres was injected into the inlet reservoir of the microfluidic chip with a pipette. To generate the electric field, a DC voltage was applied to the platinum wire electrodes placed in the two reservoirs at the ends of the channel. To investigate the effect of electric field strength on the particle motion, the applied voltage on the two electrodes was increased incrementally from 50 to 1,000 V with a high-voltage power supply (PS350, Stanford Research). The corresponding electric field was  $\sim 20$ –400 V/cm.

Figure 5 shows the observed particle behavior within the microchannels of the insulating structure for increasing electric fields. Dark areas are the solid insulators and bright areas are the microchannels filled with flowing fluorescent particles. At low electric field of 40 V/cm, streaming dielectrophoresis was observed (Fig. 5a). Streamlines of particles carried by the EOF were formed within the microchannels. Particles entered from the left of the channels, traversed the whole structure, and then exited at the right outlet. No obvious concentration of particles was observed



**Fig. 5** Concentration of green fluorescent submicron polystyrene particles in the insulating microstructures. **a–e** Depicts the concentration at different regions as the applied voltage increased. *Dark areas* are the PDMS structures, and bright (*green*) areas are the microchannels formed by the PDMS. The flow direction is from the left to the right



in this regime (streaming DEP). In the low electric field regime, drag forces on the particles from electrokinetic flow dominated the attractive effects of positive DEP and thus resulted in the streaming movement along the microchannels. As the electric field increased to 120 V/cm, trapping of particles began to occur at the right (Region 1) of the concentrator (Fig. 5b). Due to the focused electric field in this region, the DEP force began high enough to overcome the electrokinetic effects, resulting in the trapping of particles in this region. Because of the trapping, fewer particles exited the outlet. On the other hand, streaming DEP still occurred in the other regions (the left part of the concentrator). The co-existence of both streaming DEP and trapping DEP highly improved the concentration efficiency: the streaming DEP was responsible for continuously transporting of the particles from the left to the right, while trapping DEP was responsible for trapping the delivered particles. As the applied field further increased to 160 V/cm, the loss of particles at the outlet disappeared, meaning that the concentrator trapped all the incoming particles delivered by the flow (Fig. 5c). In addition, the particles were highly condensed as indicated by the intensity of the fluorescence. Similarly, trapping

DEP began to occur in 'Region 2' as the applied field increased to 200 V/cm (Fig. 5d) and occurred in 'Region 3' and 'Region 4', respectively, as the applied field increased to 240 V/cm or higher (Fig. 5e). At this point, the concentrator trapped all the particles entered from the inlet and packed them into a dense format within the microchannels. To collect the concentrated particles, the residual solution in the reservoirs was first discarded. The applied voltage was then turned off, and a pressure source (generated with a syringe) was applied from the inlet to propel the particles to the outlet reservoir. The solution collected from the concentrator was observed to contain particles in a high concentration. We also carried out experiments with particles of diameter of 500 nm (not shown). The observations were similar but required higher electric field for the same effect.

## Summary

We have demonstrated a microfluidic concentrator for rapid and efficient trapping of nanoparticles. The concentrator is composed of a series of microchannels formed by

PDMS-insulating microstructures. The applied fields were focused stepwise within the microchannels. Streaming DEP occurred at low electric fields, and trapping DEP occurred at higher electric fields. As the electric field increased, concentration of nanoparticles began to occur at different regions. Both streaming DEP and trapping DEP could simultaneously occur. The concentration was very rapid and efficient as the streaming DEP delivered particles and trapping DEP trapped the delivered particles. The proposed concentrator design can be re-configured into a format with more or less trapping regions, depending on the applications. Furthermore, the microfluidic concentrator can be implemented in applications where concentration of targets are needed, such as the concentration of cells for sample preparation and the concentration of molecular biomarkers for biological assays.

## References

1. A.E. Greenberg, L.S. Clesceri, A.D. Eaton (eds.), *Standard Methods for the Examination of Water and Wastewater*, 21st edn. (American Public Health Association, American Water Works Association and Water Environment Federation, USA, 2005)
2. D.R. Reyes et al., Micro total analysis systems. 1. Introduction, theory, and technology. *Anal. Chem.* **74**, 2623–2636 (2002)
3. M. Durr et al., Microdevices for manipulation and accumulation of micro- and nanoparticles by dielectrophoresis. *Electrophoresis* **24**, 722–731 (2003)
4. D.F. Chen, H. Du, W.H. Li, A 3D paired microelectrode array for accumulation and separation of microparticles. *J. Micromech. Microeng.* **16**, 1162–1169 (2006)
5. B.H. Lapizco-Encinas et al., Insulator-based dielectrophoresis for the selective concentration and separation of live bacteria in water. *Electrophoresis* **25**, 1695–1704 (2004)
6. M.P. Sheetz, *Laser Tweezers in Cell Biology* (New York, Academic Press, 1998)
7. A. Nilsson et al., Acoustic control of suspended particles in microfluidic chips. *Lab Chip* **4**, 131 (2004)
8. T.B. Jones, *Electromechanics of Particles* (Cambridge University Press, Cambridge, 1995)
9. D.F. Chen, H. Du, A dielectrophoretic barrier-based microsystem for separation of microparticles. *Microfluid. Nanofluid.* **3**, 603–610 (2007)
10. J.G. Kralj et al., Continuous dielectrophoretic size-based particle sorting. *Anal. Chem.* **78**, 5019–5025 (2006)
11. R. Pethig, Dielectrophoresis: using inhomogeneous AC electrical fields to separate and manipulate cells. *Crit. Rev. Biotechnol.* **16**, 331–348 (1996)
12. H.B. Li, R. Bashir, Dielectrophoretic separation and manipulation of live and heat-treated cells of *Listeria* on microfabricated devices with interdigitated electrodes. *Sens. Actuators B* **86**, 215–221 (2002)
13. Yuejun. Kang et al., DC-Dielectrophoretic separation of biological cells by size. *Biomed. Microdev.* **10**, 243–249 (2007)
14. C.-F. Chou et al., Electrodeless dielectrophoresis of single- and double-stranded DNA. *Biophys. J.* **83**, 2170–2179 (2002)
15. E.B. Cummings, A.K. Singh, Dielectrophoresis in microchips containing arrays of insulating posts: theoretical and experimental results. *Anal. Chem.* **75**, 4724–4731 (2003)